Friction stir welding of new electronic packaging materials SiCp/Al composite with T-joint

FRICTION STIR WELDING OF NEW ELECTRONIC PACKAGING MATERIALS SiCp/Al COMPOSITE WITH T-JOINT

Zeng Gao[1*] – Jianguang Feng[1] – Huanyu Yang[1]– Jukka Pakkanen[2] – Jitai Niu[1]

[1] School of Materials Science and Engineering, Henan Polytechnic University, Henan, Jiaozuo, 454003, P. R. China
[2] Institute for Materials Science and Welding, Graz University of Technology, Graz, 8010, Austria

ARTICLE INFO

***Article history*:**
Received: 26.04.2017.
Received in revised form: 13.12.2017.
Accepted: 02.02.2018.

Keywords:
SiC_p/Al composite
Microstructure
Friction stir welding
Gas tightness

DOI: *https://doi.org/10.30765/er.38.3.12*

Abstract:

Using friction stir welding, the electronic container box and lid made from aluminium matrix composites with reinforcement of SiC particle (15 vol% SiC_p/Al-MMCs) was welded successfully with T-joint. The temperature distribution of box during the process, mechanical property and microstructure of the joint as well as gas tightness of welded box was investigated. The experimental results indicated that the satisfactory T-joint can be obtained under appropriate friction stir welding parameters. During the welding process, the bottom center, which was used to place the electronic component, reached a quite lower temperature of 100°C. That can ensure safety of components in the box. After the welding process, the microstructure in stir zone was better than in base material due to the refining and homogeneous distribution of the SiC particles. The experimental results showed that the electronic container box after friction stir welding had gas tightness. The He-leakage rate was under 10^{-8} Pa•m^3/s.

1 Introduction

Aluminium-based metal matrix composites (MMCs) reinforced with the ceramic particle SiC, is an interesting structural and functional material in aerospace, motor sport, and automotive industrial fields due to its several attractive advantages over the conventional base alloy, such as high specific stiffness and strength, high thermal stability, and its superior wear resistance [1-4]. It is used as well in some other fields due to its attractive properties. For the aerospace field, material properties and structure weight are very important factors. In the aerospace field, iron-cobalt-nickel alloy Kovar and copper-tungsten alloy are the most used materials in conventional application for electronic packaging manufacturing. The reason for that is that the two kinds of materials have good thermal expansion coefficient and weldability, which means that they easily get welded by conventional seam welding technology. Obviously, the disadvantages of iron-cobalt-nickel alloy Kovar and copper-tungsten alloy are their high density and low heat conductivity coefficient [5-7]. In recent decades, according to the principle of lightweight design, the conventional packaging materials need to be replaced. For the potential application in the aerospace field, the new promising material SiC_p/Al MMCs has many kinds of merits such as high heat conductivity coefficient, low density, specific high stiffness and strength.

* Corresponding author.
E-mail address: mrgaozeng@163.com

However, regarding the joining of SiC_p/Al MMCs, it is hard to obtain defect-free welds by using conventional fusion welding methods. That deleterious reaction was observed in fusion zone between SiC particles. Liquid aluminium and irregular redistribution of the SiC particles frequently occurred, which significantly limited the joint properties of SiC_p/Al MMCs [8-10]. The main reason for that is high temperature during the conventional fusion welding. Besides, the flow of molten bath can cause irregular distribution of reinforcement.

Friction stir welding (FSW) is a relative new solid-state welding technology. It has been developed quite well over the past decades to join light alloy such as aluminium [11]. Until now, FSW bas been widely used for the welding of aluminium regular seam. The FSW is a suggestible candidate in joining SiC_p/Al MMCs since this method is a solid-state process. Hence, the brittle product such as Al_4C_3, which is produced at high temperature, is not easily generated. Moreover, due to technological characteristics, FSW can improve the distribution of SiC particle in stir zone significantly, making it more homogeneous. The researchers [12-14] also indicated that the friction stir action in composite can broke the reinforcement and make them more evenly distributed. This work mainly deals with welding of SiC_p/Al MMCs which is potentially required in aerospace electronic packaging field. The electronic container box and lid need to be welded gas tightly. Meanwhile, during welding process, the components inside of box can not be damaged because of the welding heat conduction, which requires temperature at box bottom lower than 180 °C.

2 Experimental materials and procedure

The material used in this research is 15 vol% SiC_p/Al-MMCs. For composites, the base material is A356, which has good formability. The chemical composition of the base material A356 is shown in Table 1.

Table 1. Chemical composition of A356 aluminum alloy (wt.%)

Element	Si	Fe	Cu	Mg
Content	7.0	0.12	0.10	0.45
Element	Mn	Zn	Ti	Al
Content	0.05	0.05	0.20	Balance

The box and lid as shown in Figure 1, were machined from billet of composites. In previous study, the box joint type was used. However, the joint property such as gas tightness was hard to achieve. In this research, the improved T-joint type was utilized by enlarging the lid to size of 60x60 mm^2. This allows the shoulder of FSW tool to be fully on top of box eliminating lamination of stirred material on lid. Container size is 27x27x15 mm^3 and thickness of the wall is 4 mm.

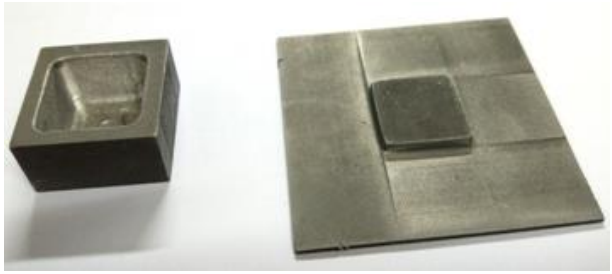

Figure 1. Shape of the box and the lid before FSW.

A MTS iSTIR BR4 friction stir welding machine was used for welding the box.

Because SiC_p/Al-MMCs is a quite wear resistant result from SiC particles existing [15], the material and the shape of FSW tool need to be considered carefully. In this research, the FSW tool is made from the material of wear resistant WC-Co. To improve the FSW tool wear resistance, a cone shape tool is used in experiment. The shape and diameter of the FSW tool are given in Figure 2.

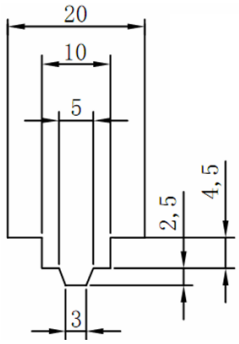

Figure 2. The FSW-tool geometry and dimension (Unit: mm).

After previous optimization, the welding parameters were: spindle speed of 1500 RPM, transitional speed 120 mm/min, pressing force 2 kN, plunge depth of 2.55 mm and tool tilt angle of 3°. T-joint geometry, the FSW tool position, as well as T-joint stereomicroscope image before and after FSW are shown in Figure 3.

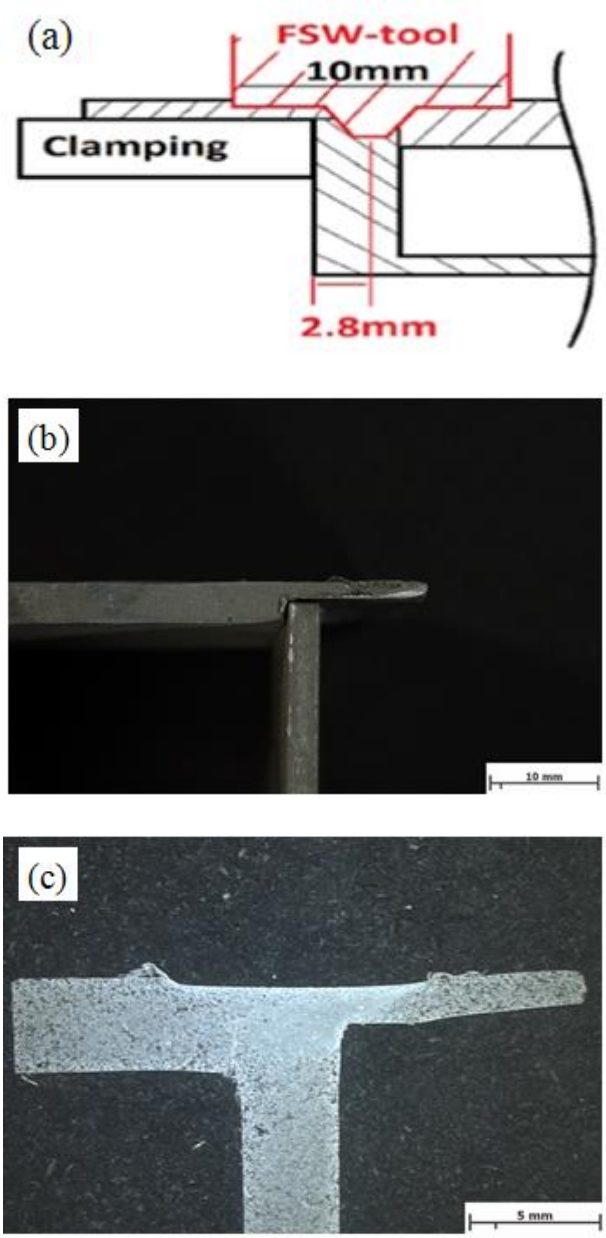

Figure 3. T-joint (a) joint geometry and the FSW-tool position, (b) image of T-joint before FSW and (c) stereomicroscope image of T-joint after FSW.

The temperatures were measured at specific points during FSW by using four pairs of chromium-nickel silicon thermocouples. Shearing test was performed at room temperature on the electronic universal testing machine (IIC-MST-100). During the shearing test, a constant shear rate of 0.2 mm/min was utilized. Weld quality was checked with light microscopy. The SEM- and EDX-analysis were made with FEI, Quanta 200 microscope and EDAX-sensor. The gas tightness test was performed on helium leak mass spectrometer KYKY ZQJ-530.

3 Results and discussion

3.1 Temperature distribution during the FSW process

To protect devices in the electronic container box, temperature at the bottom center of the box needs to be limited to less than 180 °C [16]. It is determined by melting point of soldering filler metal in chips. Therefore, temperature development during the FSW is measured from four locations from the middle of the box as shown in Figure 4. Figure 5 gives the temperature measurement results.

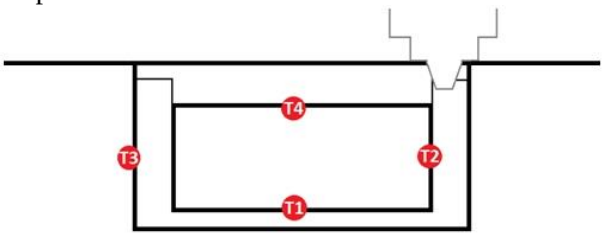

Figure 4. A cross section of the center of the box showing temperature measurements.

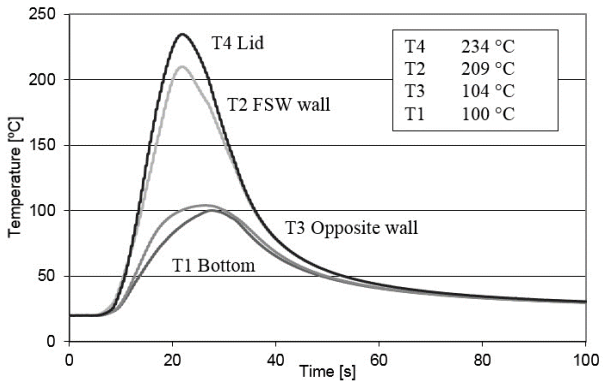

Figure 5. Temperature development during FSW and peak temperatures.

The components are placed in the bottom center of the box as shown in T1. The peak temperature during FSW at T1 is 100°C, which can guarantee the safety of the components determined by melting point of Sn-Pb solder (180°C) [16]. Because welding heat mostly comes from the FSW tool shoulder during welding, it is obviously that T4 reaches the highest temperature of 234°C. T2 is quite close to the welding center, hence it reaches the 2nd highest temperature of 209°C. Figure 5 also shows that peak

temperature at T1 and T3 and later in T4 and T2. The reason for that is that the distance of T1 and T3 is larger than that of T4 and T2.

3.2 Mechanical property of the joint

The shear test was done in 100 kN computer controlled bench. Computer was recording the force and elongation of the specimen. The sampling position for the shearing test on the box was shown in Figure 6.

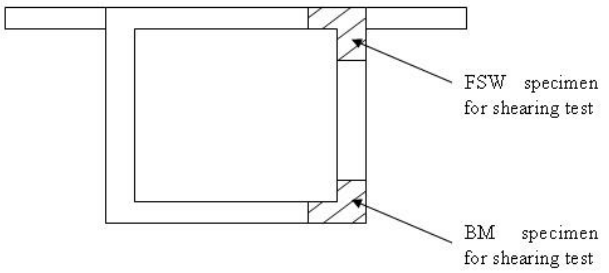

Figure 6. Sampling positions for the shearing test on the electronic container box.

For base material (BM) and FSW specimen, Figure 7 is manufactured and tested. Five specimens of BM and FSW sections were used for the shearing test. Stir zone is shown in section line region. The stir zone is in the middle and the lack of wall fusion is starting the shear.

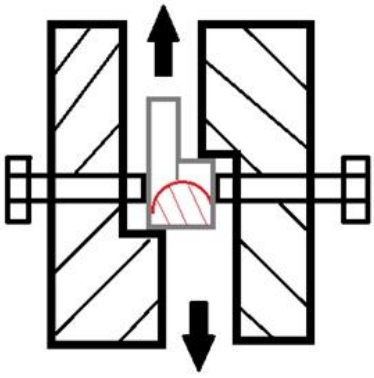

Figure 7. The shear test of FSW specimen.

To protect test fixture, the shear displacement was limited to less than 3 mm. With BM and FSW specimens, the shear test maximum force was exceeded. The FSW specimen wall-lid interface had opened but the material hadn't broken thoroughly. Regarding the BM specimen, the second shear test broke specimen with the help of plastic deformation from the first test. Joining of BM and FSW is too good to be tested with a way shown in Figure 7. With the same FSW process parameters, tensile specimen was manufactured then. In the tensile test, it can be found that breakage occurred in the base material as given in Figure 8, which means that mechanical property in the FSW joint is better than that in the base material. That has significant relationship with microstructure and particle distribution in joint of SiC_p/Al MMCs, which will be analyzed in part of the microstructure.

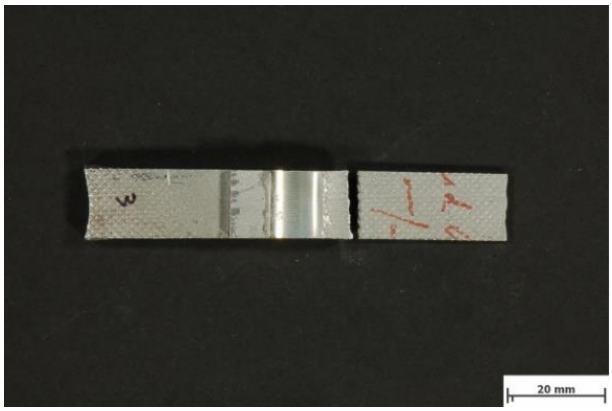

Figure 8. The tensile test result of SiC_p/Al MMCs joint.

3.3 Microstructure of the FSW joint

Figure 9 shows the box after FSW from bottom and top looking as well as the clamping device used in the experiment. After the FSW, four keyholes will be left in the box lid. However, excessive lid with keyhole will be cut away before application.

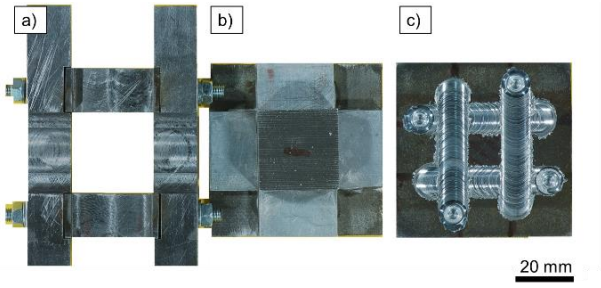

Figure 9. FSW box: (a) clamping device, (b) bottom look of FSW box and (c) top look of FSW box.

Figure 10 shows microstructure distribution of as-casted 15 vol% SiC_p/Al-MMCs used in this research. The microstructure for as-casted composite consists

of α-aluminium, eutectic Si and SiC particles. The distribution of the SiC particles in base aluminium is not very uniformed. Most of the SiC particles distribute on grain boundary of base metal. The reason for that is that during casting manufacturing, the SiC particles are pushed to the grain boundary region driving by solidification force.

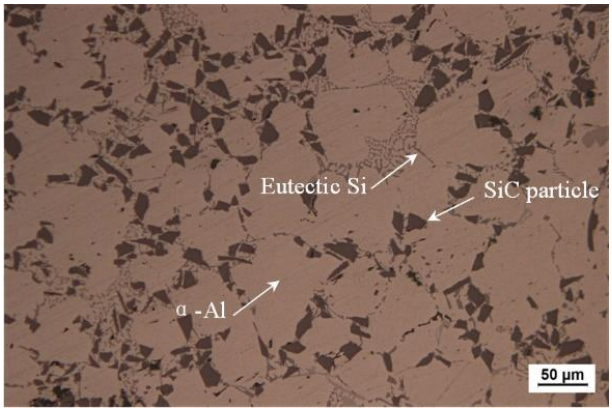

Figure 10. Microstructure of 15 vol% SiC_p/Al-MMCs.

T-joint of 15 vol% SiC_p/Al-MMCs was successfully welded by the FSW. As shown in Figure 11, microstructure of the FSW T-joint is separated into four regions: (a) stir zone (SZ); (b) thermo-mechanical affected zone (TMAZ); (c) heat affected zone (HAZ); and (d) parent material.

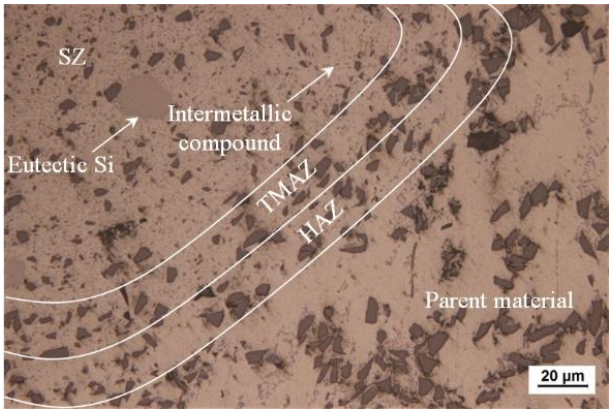

Figure 11. Microstructure of FSW joint of 15 vol% SiC_p/Al-MMCs with four zones.

Because of severe deformation and stirring during the FSW process, the SiC particles distribution in SZ becomes more even, meaning the re-arrangement of the SiC particles. Moreover, the size of the SiC particles in SZ is smaller than that in parent metal due to particle breakage during friction and stirring. It can be found that the FSW joint is free from defects such as void and groove in SZ. Meanwhile, blocky eutectic Si and precipitation product such as intermetallic phase can be observed in this area as well. The homogeneous distribution and smaller size of particle in SZ will promote joint mechanical property in this area. As is shown in tensile test, breakage occurred in base material rather than in the joint. The TMAZ, which is adjacent to SZ, has been plastically deformed and thermally affected. In TMAZ, clustered SiC particles are redistributed slightly as well. The particles distribution follows orientation of material flow in TMAZ. The HAZ between TMAZ and parent material exhibits a similar microstructure compared to base composite.

Figure 12 shows the EDX analysis points defined on SEM microstructure of composite in stir zone. Figure 12 (a) describe results of the EDX analysis which are taken from indicated points represented in fine SiC particles, Figure 12 (b) represented to matrix alloy, respectively. Figure 12 (a) shows that Si, C and Al peaks are mainly present.

Figure 13 describes SEM image in stir zone and EDX distribution maps of Al and Si in the same photograph. The EDX results highlighted element distribution of Al and Si. Al and Si are represented by red and green area, respectively. Al, Si and C distributions investigated by the EDX analysis consisted with SEM image, as shown in Figure 13 (a). The presence of coarse and fine SiC particles in SZ is also revealed by the EDX analysis of Al, Si and C.

3.4 Gas tightness of the FSW joint

Gas tightness was measured with helium leak mass spectrometer KYKY ZQJ-530. Excessive box lid was cut away before testing. Welding defects such as gap, groove, and void in joint might trap He-gas and affect gas tightness results. In the experiment, specimen was put into gas chamber that was flooded with 0.4MPa of He-gas and kept there for 30 minutes. From the chamber, an individual sample was rinsed with fresh air to remove helium gas on the surface and put into vacuum chamber. The gas analysator was at pressure of 10^-10Pa. The chamber holding the sample was made into 10^-10Pa pressure and connected to analysator. After connection, the vacuum of total system without pump was read. The vacuum drop of 4 decades indicated that the sample was not gas tight.

Testing of an empty box or a half box as shown in Figure 14 was made by putting it on top of soft vinyl plate from where was a hole to vacuum hose.

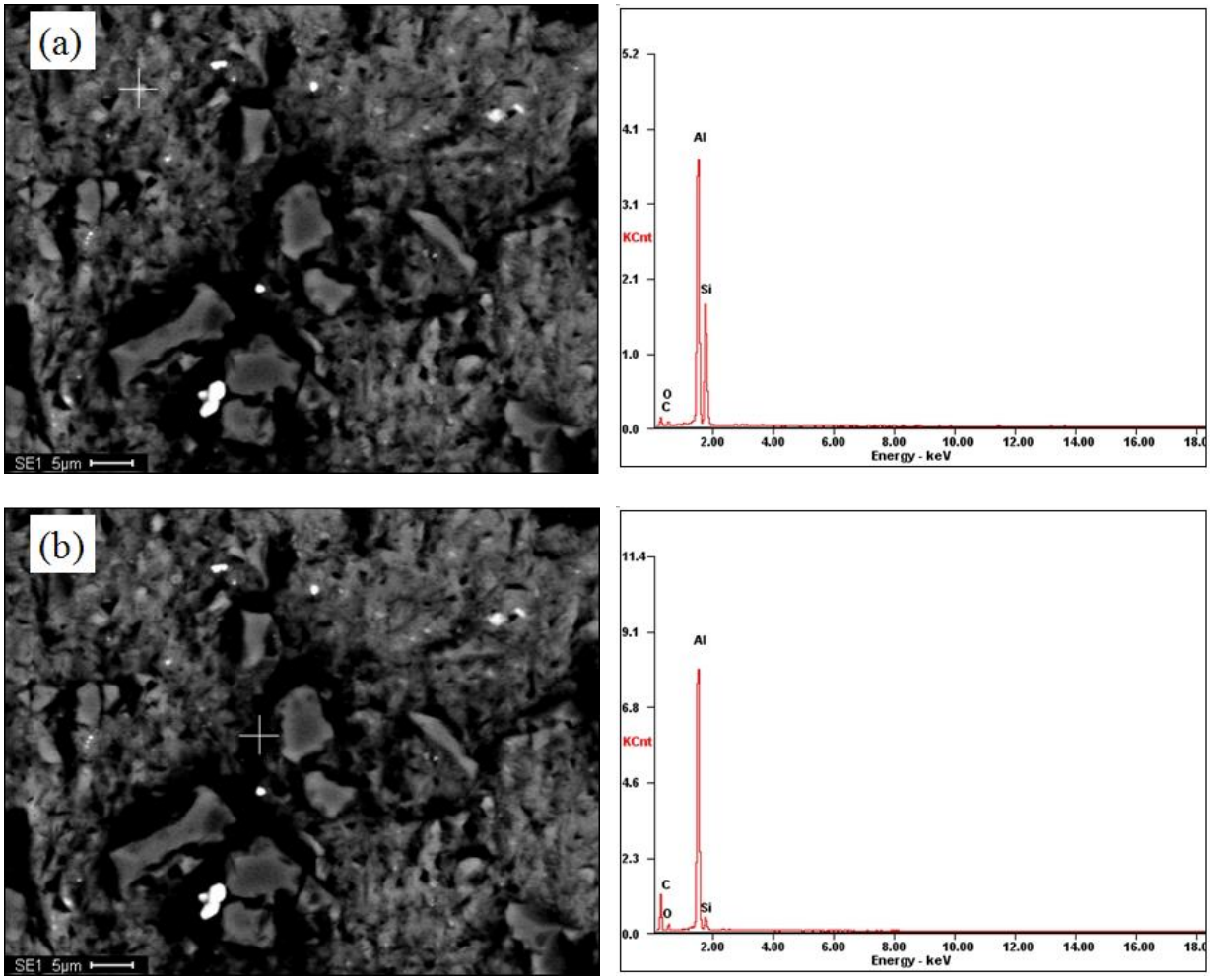

Figure 12. The SEM microstructure of the composite in stir zone and the EDX analysis results take from: (a) fine SiC particle and (b) matrix alloy

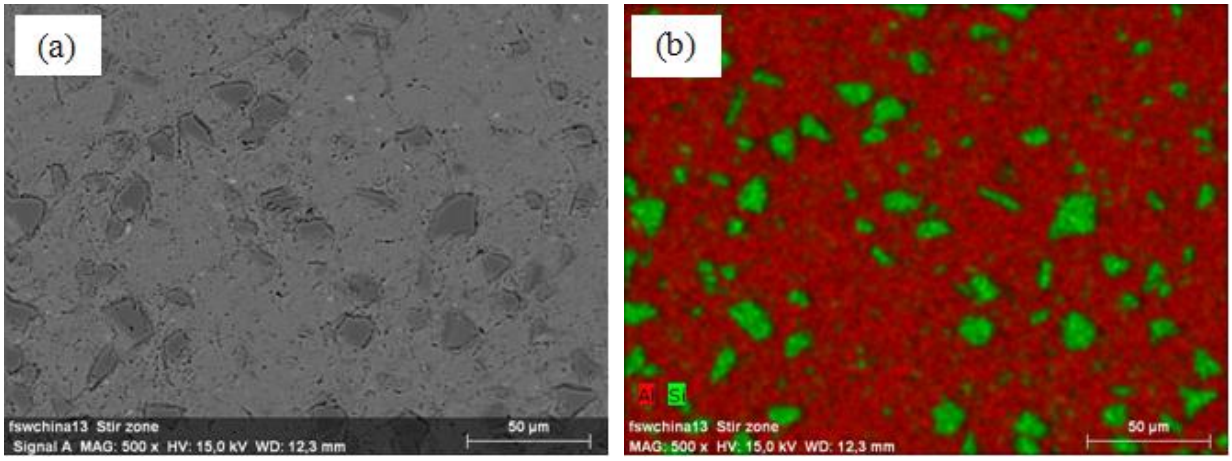

Figure 13. The SEM image of stir zone and EDX distribution maps of Al and Si in the same image: (a) The SEM microstructure of composite in stir zone, and (b) The EDX distribution map of Al (red area) and Si (green area).

Vacuum of 10^{-10} Pa was sucked from under to inside of the box. Helium gas was then sprayed on top of specimen and helium leaking through joint defect and base material was measured.

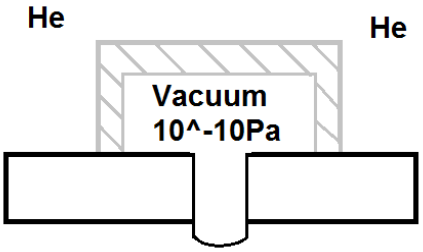

Figure 14. Gas tightness test for half box.

In the experiments, five boxes and ten half boxes were measured to examine the joint gas tightness. The mass spectrometer analysis indicated that He-leakage rates of 15 specimens were all between 10^{-8} Pa•m^3/s and 10^{-9} Pa•m^3/s, which meant that the specimens were all gas tight. Therefore, the FSW technology and process parameter in this work was appropriate for the welding of electronic packaging container made from 15 vol%, SiC_p/Al-MMCs.

4 Summary and conclusion

In this work, electronic container box made from 15 vol% SiC_p/Al-MMCs was welded by the stir welding successfully. The satisfactory joint was obtained as well. Temperature development in the box during the FSW process, mechanical property and microstructure of the joint, as well as gas tightness of the FSW box were studied.

The following conclusions can be drawn from this work:

(1) The friction stir welding is a promising candidate for joining of 15 vol%, SiC_p/Al-MMCs. For electronic packaging container, satisfied joint can be produced by the FSW technique with a T-Joint. The appropriate FSW parameters for the container box in this work are following: spindle speed of 1500 RPM, transitional speed 120 mm/min, pressing force 2 kN, plunge depth of 2.55 mm and tool tilt angle of 3°.

(2) The maximum temperature reached at the lid center is 209°C, and that in the center of friction stir welded wall is 234°C. The bottom center, which is used to place electronic components, reaches a temperature of 100°C during the whole FSW process. The process parameters can guarantee safety of the components determined by melting point of Sn-Pb solder (180°C).

(3) The SiC particles in stir zone will be broken and refined due to the friction stir welding. Some SiC particles flake to smaller pieces. Meanwhile, the distribution of the SiC particles in the stir zone is more homogeneous due to high deformation and stirring. The microstructure of 15 vol% SiC_p/Al-MMCs in the stir zone is better than that in parent material.

(4) The electronic container boxes manufactured by the FSW are gas tight. Lower He-leakage rate (between 10^{-8} Pa•m^3/s and 10^{-9} Pa•m^3/s) can be reached. The mechanical property of the FSW joint is better than that of parent material due to refining and homogeneous distribution of the SiC particles in the stir zone.

Acknowledgments

The authors thank for financial support of Henan Postdoctoral Foundation and Doctoral Foundation of Henan Polytechnic University (No. B2014-006).

References

[1] Wang, W., Li, Q., Ma, R., Cao, X., Cui, Y., Fan, Y., Yang, T., Liu, B.: *Superior bending and impact properties of SiC matrix composites infiltrated with an aluminium alloy*, Ceramics International, 43(2017), 5, 4551-4556.

[2] Hamdy, A.S., Alfosail, F., Gasem, Z.: *Eco-friendly, cost-effective silica-based protective coating for an A6092SiC17.5p aluminum metal matrix composite*, Electrochimica Acta, 89(2013), 749-755.

[3] Gao, Z., Niu, J., Yang, S., Wang, X., Cheng, D.: *Soldering of aluminum matrix composites SiCp/A356 and Kovar alloy*, Engineering Review, 33(2013), 2, 123-128.

[4] Koli, D.K., Agnihotri, G., Purohit, R.: *Advanced aluminium matrix composites: the critical need of automotive and aerospace engineering fields*, Materials Today Proceedings, 2(2015), 3032-3041.

[5] Yoon, J.W., Jung, S.B.: *Investigation of interfacial reaction between Au–Sn solder and Kovar for hermetic sealing application*, Microelectronic Engineering, 84(2007), 11, 2634-2639.

[6] Gao, Z., Chen, Z., Xu, D., Wang, P., Niu, J., Wang, X.: *Vacuum brazing between*

SiCp6063Al/MMCs and Fe-Ni alloys, Engineering Review, 36(2016), 3, 249-254.

[7] Tan, C.W., Chan, Y.C., Leung, B.N.W., Tsun, J., So, A.C.K.: *Characterization of Kovar-to-Kovar laser welded joints and its mechanical strength*, Optics & Lasers in Engineering, 43(2005), 2, 151-162.

[8] Shen, P., Wang, Y., Ren, L., Li, S., Liu, Y., Jiang, Q.z: *Influence of SiC surface polarity on the wettability and reactivity in an Al/SiC system*, Applied Surface Science, 355(2015), 930–938.

[9] Storjohann, D., Barabash, O.M., David, S.A., Sklad, P.S., Bloom, E.E., Babu, S.S.: *Fusion and friction stir welding of aluminum-metal-matrix composites*, Metallurgical and Materials Transactions A, 36(2005), 11, 3237–3247.

[10] Urena, A., Escalera, M.D., Gil, L.: *Influence of interface reactions on fracture mechanisms in TIG arc-welded aluminium matrix composites*, Composites Science & Technology, 60(2000), 4, 613–622.

[11] Staron, P., Kocak, M., Williams, S.: *Residual stresses in friction stir welded Al sheets*, Applied Physics A, 350(2002), 1, 1161-1162.

[12] Salih, O.S., Ou, H., Sun, W., Mccartney, D.G.: *A review of friction stir welding of aluminium matrix composites*, Materials & Design, 86(2015), 61-71.

[13] Fernandez, G.J., Murr, L.E.: *Characterization of tool wear and weld optimization in the friction-stir welding of cast aluminum 359+20% SiC metal-matrix composite*, Materials Characterization, 52(2004), 1, 65-75.

[14] Amirizad, M., Kokabi, A.H., Gharacheh, M.A., Sarrafi, R., Shalchi, B., Azizieh, M.: *Evaluation of microstructure and mechanical properties in friction stir welded A356+15% SiC_p cast composite*, Materials Letters, 60(2006), 4, 565-568.

[15] Bist, A., Saini, J.S., Sharma, B.: *A review of tool wear prediction during friction stir welding of aluminium matrix composite*, Transactions of Nonferrous Metals Society of China, 26(2016), 8, 2003-2018.

[16] Wu, G., Zhang, Q., Chen, G., Jiang, L., Xiu, Z.: *Properties of high reinforcement-content aluminum matrix composite for electronic packages*, Journal of Materials Science: Materials in Electronics, 14(2003), 1, 9-12.